Published in final edited form as:

J Am Chem Soc. 2016 December 14; 138(49): 15801–15804. doi:10.1021/jacs.6b08376.

Probing Hydronium Ion Histidine NH Exchange Rate Constants in the M2 Channel via Indirect Observation of Dipolar-Dephased ^{15}N Signals in Magic-Angle-Spinning NMR

Riqiang Fu[*,†], **Yimin Miao**[§], **Huajun Qin**[§], and **Timothy A. Cross**[†,§]

[†]National High Magnet Field Lab, 1800 East Paul Dirac Drive, Tallahassee, Florida 32310, United States

[§]Department of Chemistry and Biochemistry, Florida State University, Tallahassee, Florida 32306, United States

Abstract

Water–protein chemical exchange in membrane-bound proteins is an important parameter for understanding how proteins interact with their aqueous environment, but has been difficult to observe in membrane-bound biological systems. Here, we demonstrate the feasibility of probing specific water–protein chemical exchange in membrane-bound proteins in solid-state MAS NMR. By spin-locking the ^{1}H magnetization along the magic angle, the ^{1}H spin diffusion is suppressed such that a water–protein chemical exchange process can be monitored indirectly by dipolar-dephased ^{15}N signals through polarization transfer from ^{1}H. In the example of the Influenza A full length M2 protein, the buildup of dipolar-dephased ^{15}N signals from the tetrad of His37 side chains have been observed as a function of spin-lock time. This confirms that hydronium ions are in exchange with protons in the His37 NH bonds at the heart of the M2 proton conduction mechanism, with an exchange rate constant of ~1750 s^{-1} for pH 6.2 at −10 °C.

Biological membranes are composed of crowded membrane-bound proteins/peptides in a lipid environment.[1] They exhibit diverse shapes and conduct many essential biological processes, such as inter- and intracellular signal transduction, protein localization, and trafficking required synergistic effects between the proteins and their surrounding complex lipid environs.[2–4] It has become clear that the membrane lipids have profound impacts on the structure and function of membrane-bound proteins and peptides.[5–9] The implications of the lipid–protein interactions have been increasingly recognized in past years and many solid-state NMR techniques have been developed to study such lipid–protein

[*]Corresponding Author: rfu@magnet.fsu.edu.

ORCID

Riqiang Fu: 0000-0003-0075-0410

Notes

The authors declare no competing financial interest.

Supporting Information

The Supporting Information is available free of charge on the ACS Publications website at DOI: 10.1021/jacs.6b08376. Materials and experimental details; derivation of Solomon equations; control experiments; brief discussion on HETCOR; ^{15}N MAS NMR spectra; modeled His37 orientations upon breaking of the H-bond (PDF)

interactions.[10–14] For instance, the influence of proteins on membrane lipid dynamics and vice versa could be investigated through deuterium line-shapes[15,16] or by relaxation parameters.[17,18] Spin diffusion from lipids into membrane proteins allows for the detection of nuclear spin magnetization in proteins for the direct investigation of lipid–protein interactions.[19–22] Magic-angle-spinning (MAS) recoupling techniques[23] are also commonly used for measuring distances from the lipid head groups to specific sites on proteins so as to study the insertion and alignment of the proteins/peptides into the lipids.[24–26] Water–protein chemical exchange[27–31] is another important parameter in the dynamic relationship between proteins and their surrounding environment that has been investigated in the past primarily through ^{1}H-^{15}N heteronuclear correlation (HETCOR) experiments.[32–34] Direct observation of water–protein exchange is challenging in the presence of strong ^{1}H spin diffusion associated with the relatively rigid membrane-bound protein environments. Here, we propose one-dimensional (1D) chemical exchange measurements for probing the specific water–protein chemical exchange kinetics of membrane-bound proteins using the Influenza A full length M2 protein (M2FL).

The M2 protein is a 97-residue membrane protein that assembles as a tetrameric bundle that conducts protons at a slow rate (10^{2}–10^{3}/s) when activated at low pH.[35,36] There are two debated proton transport mechanisms: (1) the proton is transferred through the breaking and reforming of H-bonds between two pairs of His37 dimers[27,37] or (2) individual His37 residue shuttles protons through imidazole ring reorientations and exchanging protons with water without the process of forming intermonomer His37 H-bonds.[29,30] M2 spectra dramatically vary depending on the M2 constructs and lipids used in sample preparation. For instance, a set of two resonances for His37 was observed in the conductance domain M2 (22-62) in DOPC/DOPE lipids[38] and M2(18-60) in POPC and DPhPC,[39–42] as well as the M2FL protein in *Escherichia coli* membranes,[43] suggesting that the histidine tetrad exhibits a dimer of dimer conformation. However, the M2 conductance domain M2(22-62) in viral-envelope-mimetic lipid membranes shows a single set of His37 resonances and did not bind amantadine.[29] Nevertheless, the ^{1}H-^{15}N HETCOR spectra from either the M2FL in DOPC/DOPE[31] or the truncated M2 protein in viral-envelope-mimetic lipid membranes[30] show correlations between water and His37 imidazolium nitrogen. These results indicate that water molecules are involved in proton conductance, although their interpretations yielded different conductance mechanisms. A direct measurement of the water–protein chemical exchange may shed light onto how the water with hydronium ions interacts with the protons in the His37 tetrad.

Figure 1a shows schematics for water–protein chemical exchange, where M represents water molecules, I is the specific proton in the protein that chemically exchanges with hydronium ions at an exchange rate constant of k_{IM}, and S is a spin such as ^{15}N that covalently bonds with the specific proton. With the hydronium ion concentration p in the pool of M, the exchange rate constant k_{MI} from M to I is pk_{IM}. Thus, the exchange process can be characterized by the classical Solomon equations[44] when the ^{1}H magnetization is spin-locked for a period of time t_{SL} along the magic angle (MA) by a Lee–Goldburg (LG) sequence:[45]

$$\frac{\mathrm{d}M(t_{SL})}{\mathrm{d}t_{SL}}=-\left(\frac{1}{T_{1\rho}^{M}}+pk_{IM}\right)M(t_{SL})+k_{IM}I(t_{SL}) \quad (1)$$

$$\frac{\mathrm{d}I(t_{SL})}{\mathrm{d}t_{SL}}=pk_{IM}M(t_{SL})-\left(\frac{1}{T_{1\rho}^{I}}+k_{IM}\right)I(t_{SL}) \quad (2)$$

Here, M and I represent the ^{1}H magnetizations along the MA for water and specific protein protons, respectively. The cross relaxation among protons is neglected because the ^{1}H spin diffusion is sufficiently suppressed along the MA[45] (Figures S1 and S2). For simplicity, we assume that the M and I protons have the same spin–lattice relaxation time in the LG spin-lock (LGSL) field, i.e., $T_{1\rho}^{M}=T_{1\rho}^{I}=T_{1\rho}^{H}$.

Figure 1b shows the pulse sequence for probing the specific water–protein chemical exchange through indirect observation of ^{15}N signals. After ^{1}H excitation, a rotational-echo double-resonance (REDOR)[23] based dipolar dephasing scheme is used to prepare the initial ^{1}H magnetizations, $M(0)$ and $I(0)$. A 35.3° pulse flips the ^{1}H magnetizations to the MA, followed by a LG sequence[45] to spin-lock the ^{1}H magnetizations, during which the water–protein chemical exchange takes place. The S spin is then brought into a short contact with the I protons by applying the ramped rf field on the S spin such that the cross-polarization (i.e., LGCP) is established to transfer the I magnetization into the S spins.[46,47] Thus, $I(t_{SL})$ can be monitored indirectly by its nearby S spins as a function of t_{SL}.

Without dephasing $I(0)$, as documented in eq S9, $I(t_{SL})$ contains the chemical exchange term that is scaled by the population difference between the hydronium ions and the specific proton involved in the chemical exchange, and thus is not sensitive to their exchange process. When $I(0)$ is dephased by REDOR before LGSL, $I(t_{SL})$ is derived as

$$I(t_{SL})=pM(0)\{1-\exp[-(p+1)k_{IM}t_{SL}]\}\exp(-t_{SL}/T_{1\rho}^{H})/(p+1) \quad (3)$$

Clearly, $I(t_{SL})$ builds up through the chemical exchange process k_{IM} and is proportional to the population of the hydronium ions in water, as shown in Figure 1c.

Figure 2 shows the ^{15}N spectra of the His37-labeled M2FL in lipid bilayers at −10 °C using Figure 1b. Clearly, the ^{15}N spectra (black) without ^{15}N dephasing show similar line-shapes and intensities at different t_{SL} values. With a short LGCP contact time (i.e., 200 μs), the ^{15}N signals were only cross-polarized from the protonated ^{15}N sites of His37 side chains (i.e., the τ state Nε2τ and the charged state Nδ1+ and Nε2+). The nonprotonated τ state Nδ1τ could hardly be polarized (Figure S3). These observed ^{15}N resonances are spread from 165 to ~200 ppm, whereas their correlated ^{1}H frequencies extend up to 19 ppm.[31] Such high ^{15}N and ^{1}H frequencies indicate the formation of short imidazole–imidazolium H-bonds.[48]

When the ^{15}N selective dephasing was applied, those protons that directly bond with ^{15}N become null before the LGSL so that their bonded ^{15}Ns will not be polarized. As shown in the red spectra of Figure 2, the ^{15}N signals were largely reduced at a short t_{SL}. Clearly from Figure 2, much of the spectral intensity that appears at ~165 ppm in black were not observed in red even when t_{SL} was long, indicating that these signals at ~165 ppm belong to N$\varepsilon 2\tau$ that is less accessible by the hydronium ions. This assignment was confirmed by the ^{15}N-^{15}N correlation spectrum (Figure S4). It is clear from the red spectra in Figure 2 that the dipolar-dephased ^{15}N signals from the charged His37 Nδ1+ or Nε2+ gained more intensity as t_{SL} increased, implying that their bonded protons gain magnetization during the LGSL. As ^{1}H spin diffusion is suppressed during the LGSL and any relayed transfer is largely eliminated, the observed gain can only be facilitated by chemical exchange between this particular proton and the hydronium ions. It is worth noting that, since the protons of the charged His37 H-Nδ1+ and H-Nε2+ sites were dephased at the beginning of the LGSL, no signals from the charged His37 Nδ1+ or Nε2+ protons were expected. However, in the presence of the water–protein exchange, the proton from the charged His37 H-Nδ1+ or H-Nε2+ (presumably H-Nε2+) was re-energized during the LGCP, such that the signals from the charged His37 Nδ1+ or Nε2+ are still observed. For a given LGCP contact time, these signals strongly depend on the exchange rate constant between the water and the specific proton involved. In addition, any incomplete HN dephasing by REDOR, due to various NH bond lengths, also attribute to these initial signals. Therefore, for the indirect observation via LGCP, eq 3 should be modified to include an additional constant, whose value depends on the exchange rate constant and the LGCP contact time. When the exchange is faster than the LGCP contact time, the dipolar-dephased $I(0)$ reaches its exchange equilibrium, such that $I(t_{SL})$ no longer depends on t_{SL}. Shown in Figure S5, the dipolar-dephased ^{15}N signals for the His37-labeled M2FL (pH 6.2) at +23 °C were almost identical at t_{SL} = 100 and 1000 μs, except for the N$\varepsilon 2\tau$ resonance at ~165 ppm that gains in intensity as t_{SL} increases. This implies that the N$\varepsilon 2\tau$ site in the His37 tetrad becomes accessible to water at +23 °C, whereas the protons in the His37 NH bonds exchange rapidly with hydronium ions, whose exchange rate constant could be estimated by the LGCP contact time used in the experiments, i.e., 1/200 μs = 5000 s^{-1}.

A series of 1D dipolar-dephased ^{15}N signals obtained here allows us to monitor the transient water–protein chemical exchange processes. Figure 3 shows the plot of the dipolar-dephased ^{15}N signals versus t_{SL}. We obtained $T_{1\rho}^{H}=16.2\ \mathrm{ms}$ in separate experiments and then fitted eq 3 to yield $(1 + p)k_{IM}$ = 1750 ± 552 s^{-1}. The concentration p of the hydronium ions in the M2 channel pore is about 10^{-6}M with the assumption that the pH in the pore is the same as in the bulk environment. Thus, the exchange rate constant between hydronium ions and the protons in the His37 NH bonds for the M2FL is on the order of 1750 ± 552 s^{-1} at −10 °C. This represents an average value over a number of different His37 states with various exposures to hydronium ions.

Figure 4 shows a model for the water–protein exchange process for the His37 NH bonds at the heart of the His37 tetrad. The “initial” NH protons in the His tetrad are colored green and blue for the His C–D pair. The hydronium ion is attracted by the nonprotonated Nδ1 site resulting in both His37 residues in a dimer becoming charged. The hydronium ion based

proton is colored red. These two imidazolium residues conformationally rearrange, due to charge repulsion with the newly protonated Nδ1+H site oriented toward the pool of externally exposed waters, whereas the original Nε2+H and the newly formed Nε2+H are both exposed to waters of the viral interior (Figure S6). The return of the His Nδ1+H proton to the waters of the viral exterior results in a futile cycle, while the absorbance of either His Nε2+H protons by waters of the viral interior results in a successful transport of a proton across the membrane. If the proton in the original imidazole-imidazolium H-bond is reabsorbed by water (right-hand path), the imidazolium donates its H-Nδ1 proton to reform the same His37 C–D pair with an imidazolium-imidazole H-bond utilizing a π state. This proton rapidly rearranges crossing the H-bond barrier to form a τ-charge H-bonded pair, back to the original state. When an interior water reabsorbs the proton of the newly formed Nε2+H, D becomes a π state and forms a new imidazolium-imidazole H-bond with H-Nδ1 of His A (left-hand path) with the proton rapidly crossing the H-bond barrier to form a τ-charge hydrogen bonded pair, leading to a rotation of the imidazolium-imidazole bonding pairs[37] (Figure 7S). This continual process for bringing the hydronium protons into the His37 NH is essential for the buildup of the dipolar-dephased ^{15}N signals as a function of t_{SL}. Thus, the buildup of the dipolar-dephased ^{15}N signals, as observed here, discriminates the proton shuttling mechanism[29,30] from the hydronium pore mechanism in the M2FL proton channel in lipid bilayers.

In summary, we have demonstrated the feasibility of probing specific water–protein chemical exchange in membrane-bound proteins via indirect observation of dipolar-dephased ^{15}N signals in solid-state MAS NMR by spin-locking the ^{1}H magnetization along the MA. Although hydrogen–deuterium exchange[49] characterizes the accumulation of a slow exchange process, here the dynamics on a sub-microsecond scale are documented for this proton transport mechanism. By suppressing the ^{1}H spin diffusion, the pure chemical exchange during the LGSL is monitored. To the best of our knowledge, this is the first direct observation of kinetic water–protein chemical exchange processes on the submsec time scale in membrane-bound proteins/peptides. Thus, this new technique provides an opportunity to characterize structure–function relationships of membrane-bound species at the water–bilayer interface, and in particular to understand the nature of how H-bonds are formed and broken in biological systems during proton transport in the M2 proton channel or other transporters.

Supplementary Material

Refer to Web version on PubMed Central for supplementary material.

Acknowledgments

This work was supported by NIH grants AI023007 and AI119178. All NMR experiments were performed at the National High Magnetic Field Lab supported by the NSF Cooperative agreement DMR-1157490 and the State of Florida.

References

1. Dupuy AD, Engelman DM. Proc Natl Acad Sci U S A. 2008; 105:2848. [PubMed: 18287056]
2. McMahon HT, Gallop JL. Nature. 2005; 438:590. [PubMed: 16319878]

3. Groves JT, Kuriyan J. Nat Struct Mol Biol. 2010; 17:659. [PubMed: 20495561]
4. Schmick M, Bastiaens PIH. Cell. 2014; 156:1132. [PubMed: 24630717]
5. Brown MF. Chem Phys Lipids. 1994; 73:159. [PubMed: 8001180]
6. Mitchell DC, Niu SL, Litman BJ. Lipids. 2003; 38:437. [PubMed: 12848291]
7. Soubias O, Gawrisch K. Biochim Biophys Acta, Biomembr. 2012; 1818:234.
8. Zhou HX, Cross TA. Annu Rev Biophys. 2013; 42:361. [PubMed: 23451886]
9. Cross TA, Murray DT, Watts A. Eur Biophys J. 2013; 42:731. [PubMed: 23996195]
10. Cross TA, Sharma M, Yi M, Zhou HX. Trends Biochem Sci. 2011; 36:117. [PubMed: 20724162]
11. Duerr UHN, Gildenberg M, Ramamoorthy A. Chem Rev. 2012; 112:6054. [PubMed: 22920148]
12. Miao Y, Cross TA. Curr Opin Struct Biol. 2013; 23:919. [PubMed: 24034903]
13. Huster D. Biochim Biophys Acta, Mol Cell Biol Lipids. 2014; 1841:1146.
14. Krepkiy D, Gawrisch K, Swartz KJ. J Mol Biol. 2012; 423:632. [PubMed: 22858867]
15. Watts A. Biochim Biophys Acta, Rev Biomembr. 1998; 1376:297.
16. Bechinger B, Salnikov ES. Chem Phys Lipids. 2012; 165:282. [PubMed: 22366307]
17. Huster D. Prog Nucl Magn Reson Spectrosc. 2005; 46:79.
18. Trouard TP, Nevzorov AA, Alam TM, Job C, Zajicek J, Brown MF. J Chem Phys. 1999; 110:8802.
19. Huster D, Yao Y, Hong M. J Am Chem Soc. 2002; 124:874. [PubMed: 11817963]
20. Li SH, Su YC, Luo WB, Hong M. J Phys Chem B. 2010; 114:4063. [PubMed: 20199036]
21. Sergeyev IV, Bahri S, Day LA, McDermott AE. J Chem Phys. 2014; 141:22D533.
22. Paulson EK, Morcombe CR, Gaponenko V, Dancheck B, Byrd RA, Zilm KW. J Am Chem Soc. 2003; 125:14222. [PubMed: 14624539]
23. Gullion T, Schaefer J. J Magn Reson. 1989; 81:196.
24. Harada E, Todokoro Y, Akutsu H, Fujiwara T. J Am Chem Soc. 2006; 128:10654. [PubMed: 16910640]
25. Chekmenev EY, Jones SM, Nikolayeva YN, Vollmar BS, Wagner TJ, Gor'kov PL, Brey WW, Manion MN, Daugherty KC, Cotten M. J Am Chem Soc. 2006; 128:5308. [PubMed: 16620079]
26. Eddy MT, Ong TC, Clark L, Teijido O, van der Wel PCA, Garces R, Wagner G, Rostovtseva TK, Griffin RG. J Am Chem Soc. 2012; 134:6375. [PubMed: 22435461]
27. Hu J, Fu R, Nishimura K, Zhang L, Zhou HX, Busath DD, Vijayvergiya V, Cross TA. Proc Natl Acad Sci U S A. 2006; 103:6865. [PubMed: 16632600]
28. Fu R, Gordon ED, Hibbard DJ, Cotten M. J Am Chem Soc. 2009; 131:10830. [PubMed: 19621928]
29. Hu F, Schmidt-Rohr K, Hong M. J Am Chem Soc. 2012; 134:3703. [PubMed: 21974716]
30. Hong M, Fritzsching KJ, Williams JK. J Am Chem Soc. 2012; 134:14753. [PubMed: 22931093]
31. Miao Y, Fu R, Zhou HX, Cross TA. Structure. 2015; 23:2300. [PubMed: 26526851]
32. Harbison GS, Roberts JE, Herzfeld J, Griffin RG. J Am Chem Soc. 1988; 110:7221.
33. Bockmann A, Juy M, Bettler E, Emsley L, Galinier A, Penin F, Lesage A. J Biomol NMR. 2005; 32:195. [PubMed: 16132820]
34. Lesage A, Emsley L, Penin F, Bockmann A. J Am Chem Soc. 2006; 128:8246. [PubMed: 16787089]
35. Sugrue RJ, Hay AJ. Virology. 1991; 180:617. [PubMed: 1989386]
36. Sakaguchi T, Tu QA, Pinto LH, Lamb RA. Proc Natl Acad Sci U S A. 1997; 94:5000. [PubMed: 9144179]
37. Sharma M, Yi M, Dong H, Qin H, Peterson E, Busath DD, Zhou HX, Cross TA. Science. 2010; 330:509. [PubMed: 20966252]
38. Can TV, Sharma M, Hung I, Gor'kov PL, Brey WW, Cross TA. J Am Chem Soc. 2012; 134:9022. [PubMed: 22616841]
39. Andreas LB, Eddy MT, Pielak RM, Chou JJ, Griffin RG. J Am Chem Soc. 2010; 132:10958. [PubMed: 20698642]
40. Andreas LB, Eddy MT, Chou JJ, Griffin RG. J Am Chem Soc. 2012; 134:7215. [PubMed: 22480220]

41. Colvin MT, Andreas LB, Chou JJ, Griffin RG. Biochemistry. 2014; 53:5987. [PubMed: 25184631]
42. Andreas LB, Reese M, Eddy MT, Gelev V, Ni QZ, Miller EA, Emsley L, Pintacuda G, Chou JJ, Griffin RG. J Am Chem Soc. 2015; 137:14877. [PubMed: 26218479]
43. Miao Y, Qin H, Fu R, Sharma M, Can TV, Hung I, Luca S, Gor'kov PL, Brey WW, Cross TA. Angew Chem. 2012; 124:8508.
44. Stejskal, EO., Memory, JD. High Resolution NMR in the Solid State - Fundamentals of CP/MAS. Oxford University Press; Oxford: 1994.
45. Lee M, Goldburg W. Phys Rev. 1965; 140:A1261.
46. Fu R, Hu J, Cross TA. J Magn Reson. 2004; 168:8. [PubMed: 15082244]
47. Hong M, Yao YX, Jakes KS, Huster D. J Phys Chem B. 2002; 106:7355.
48. Eckert H, Yesinowski JP, Silver LA, Stolper EM. J Phys Chem. 1988; 92:2055.
49. Tian CL, Gao PF, Pinto LH, Lamb RA, Cross TA. Protein Sci. 2003; 12:2597. [PubMed: 14573870]

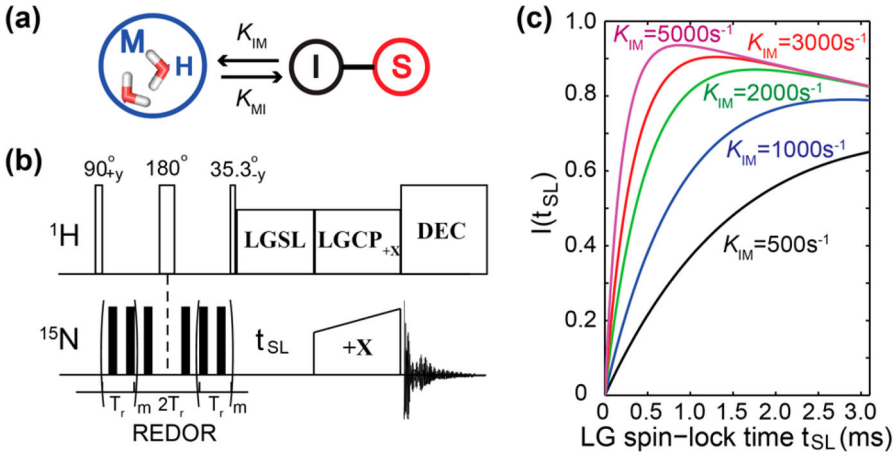

Figure 1.

(a) Schematics for the water–protein chemical exchange system. (b) Pulse sequence used to probe specific water–protein exchange via indirect ^{15}N observation. (c) Simulated buildups of the dipolar-dephased ^{1}H magnetization I as a function of t_{SL} at various exchange rate constants k_{IM}, using $T_{1\rho}^{H}$=16.2 ms and $p = 10^{-6}$.

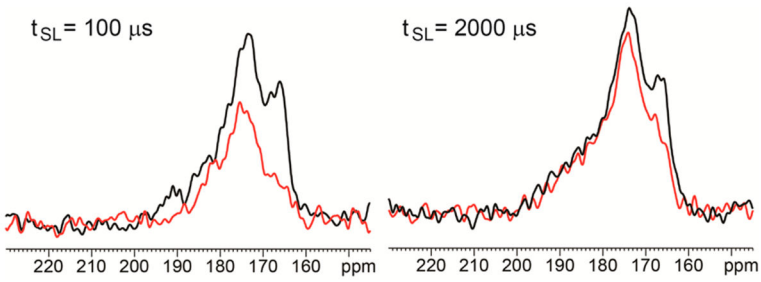

Figure 2.

Expanded ^{15}N spectra of the His37-labeled M2FL (pH 6.2) in lipid bilayers at −10 °C without (black) and with (red) ^{15}N-dipolar dephasing at t_{SL} of 100 and 2000 μs.

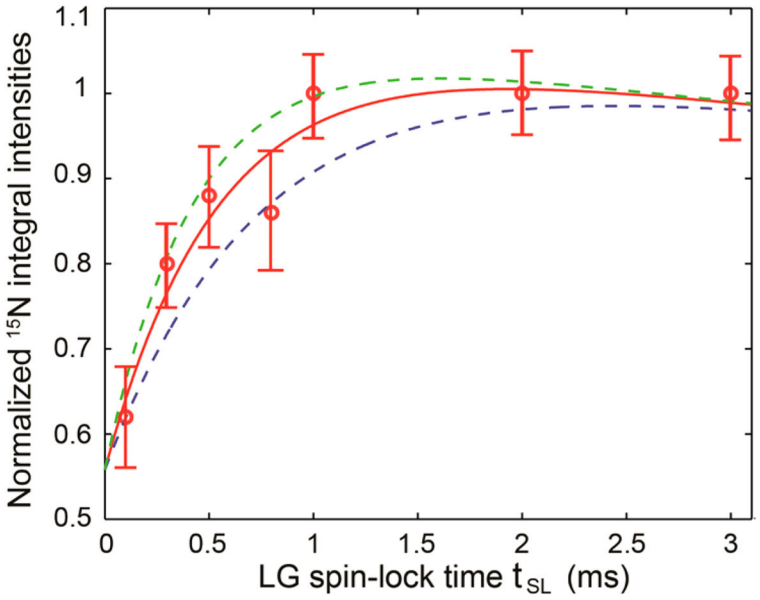

Figure 3.

Normalized dipolar-dephased ^{15}N integral intensities as a function of t_{SL} for the His37-labeled M2FL (pH 6.2) at −10 °C. The red line represents the fitting curve with k_{IM} = 1750 s^{-1}. The dashed green and blue lines are the curves for k_{IM} = 2250 and 1250 s^{-1}, respectively.

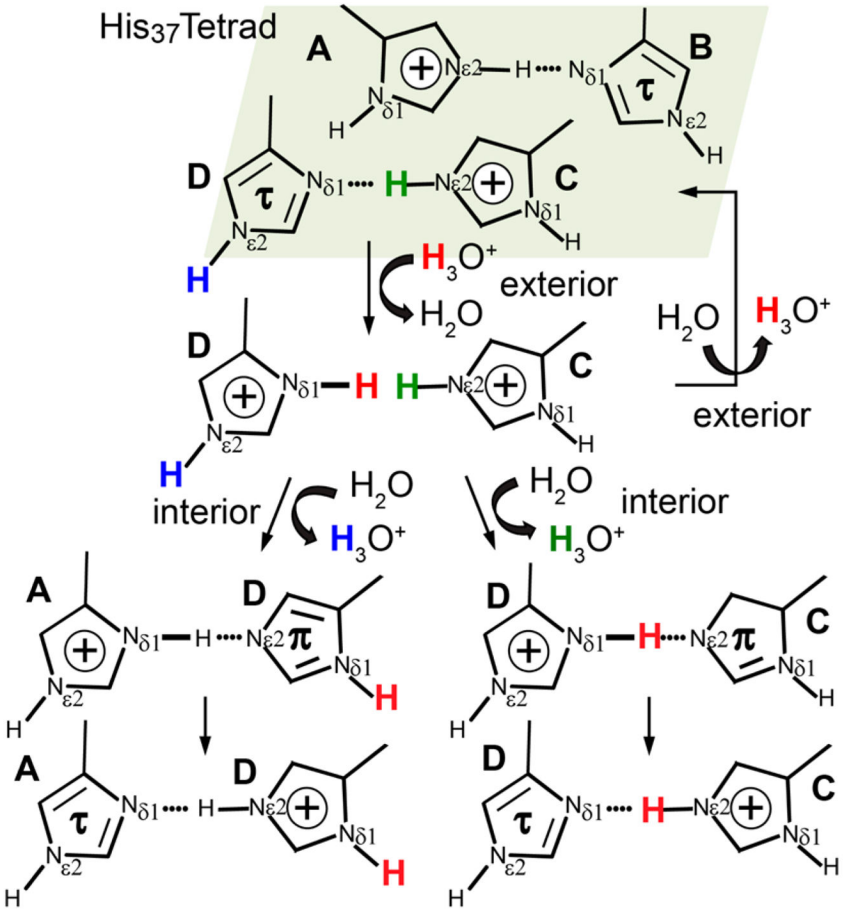

Figure 4.
Chemical exchange model between water and the NH protons in the His37 tetrad of the M2 proton channel.